Journal of Southeast University (English Edition) Vol. 41, No. 1, pp. 109-117 Mar. 2025 ISSN 1003-7985

A novel wire arc additive and subtractive hybrid manufacturing process optimization method

GUO Yiming[1], ZHANG Wanyuan[1], XIAO Mingkun[1], SONG Shida[2], ZHANG Xiaoyong[2]

(1. School of Mechanical Engineering, Nanjing University of Science and Technology, Nanjing 210094, China;
2. School of Materials Science and Engineering, Nanjing University of Science and Technology, Nanjing 210094, China)

Abstract: A reasonable process plan is an important basis for implementing wire arc additive and subtractive hybrid manufacturing (ASHM), and a new optimization method is proposed. Firstly, the target parts and machining tools are modeled by level set functions. Secondly, the mathematical model of the additive direction optimization problem is established, and an improved particle swarm optimization algorithm is designed to decide the best additive direction. Then, the two-step strategy is used to plan the hybrid manufacturing alternating sequence. The target parts are directly divided into various processing regions; each processing region is optimized based on manufacturability and manufacturing efficiency, and the optimal hybrid manufacturing alternating sequence is obtained by merging some processing regions. Finally, the method is used to outline the process plan of the designed example model and applied to the actual hybrid manufacturing process of the model. The manufacturing result shows that the method can meet the main considerations in hybrid manufacturing. In addition, the degree of automation of process planning is high, and the dependence on manual intervention is low.

Key words: wire arc additive manufacturing; hybrid manufacturing; process optimization; manufacturability

DOI: 10.3969/j.issn.1003-7985.2025.01.014

Wire arc additive manufacturing (WAAM) has the advantages of high deposition rates, low manufacturing costs, and theoretically unlimited build volumes, which are frequently adopted in the additive manufacturing of large-sized and complex components[1-2]. However, WAAM is a complex physical and chemical process, specifically in the form of continuous thermal cycling, continuous accumulation of heat, and obvious flow behavior of the molten pool, which limits its application in the manufacturing of large-sized and complex parts. Therefore, scholars at home and abroad have investigated WAAM from various perspectives in recent years, mainly including the microstructure and mechanical properties of typical materials[3-4], process parameters[5], process planning[6], and auxiliary process[7-8], providing a reference for improving the forming effect of WAAM in practical applications. Composite manufacturing with additive and subtractive processes is also an effective method for solving the problem.

In recent years, additive and subtractive hybrid manufacturing (ASHM) has been investigated and applied in several fields; however, challenges, especially for parts with complex structures, still exist. Thus, the selection of a reasonable manufacturing scheme, which is influenced by suspended structures, manufacturability, and processing efficiency, is crucial[9]. Process optimization is adopted to subdivide parts and determine the sequence of interlaced ASHM operations; however, it still encounters difficulties. A reasonable processing scheme can not only improve processing quality and efficiency but also serve as a critical prerequisite for residual stress/distortion assessment and control[10-11]. In practice, the optimization of additive and subtractive processes is usually performed manually, which heavily relies on the experience and knowledge of operators. This work is extremely time-consuming and encounters difficulties in obtaining the optimal solution. Therefore, an effective optimization algorithm for the ASHM is urgently needed. The process planning of additive manufacturing has been extensively investigated. Zhao et al. [12] proposed an innovative WAAM process planning strategy by considering thermal behavior, which can improve the deposition quality. Das et al. [13] designed a computer-aided process planning approach to fabricate functional components. Most of the existing research on ASHM first uses additive manufacturing to build an entire near net shape and then performs subtractive processing, which is difficult to apply to the complex part processing and inapplicable to the ASHM. The in-situ forming of complex parts can be achieved through the alternation of multiple additive and subtractive processes. Research on process optimization of the ASHM is currently in the early stages. Behandish et al. [14] proposed an automated additive-subtrac-

Received 2024-05-10, **Revised** 2024-08-07.

Biography: Guo Yiming (1993—), male, doctor, lecturer, ymguo@njust.edu.cn.

Foundation items: The National Natural Science Foundation of China (No. 52305381), the Natural Science Foundation of Jiangsu Province (No. BK20210351), the Fundamental Research Funds for the Central Universities (No. 30923011008).

Citation: GUO Yiming, ZHANG Wanyuan, XIAO Mingkun, et al. A novel wire arc additive and subtractive hybrid manufacturing process optimization method[J]. Journal of Southeast University (English Edition), 2025, 41(1): 109-117. DOI: 10.3969/j.issn.1003-7985.2025.01.014.

tive process optimization algorithm to optimize the cost of hybrid manufacturing. Soonjo et al. [15] used the recursive volume decomposition to determine the optimal sequence of ASHM. The aforementioned studies used manufacturability as a constraint to reduce the costs of ASHM. However, the suspended structure and tool accessibility make it difficult to obtain a reasonable processing scheme. In this study, a novel process optimization method for ASHM is proposed. First, the target parts and machining tools are implicitly modeled to obtain positional information in the machining space. Then, an improved particle swarm optimization (PSO) algorithm is developed to determine the part orientation for minimizing the support volume and manufacturing costs. Finally, a process optimization approach is proposed by considering the manufacturability and efficiency. The effectiveness of the proposed method is verified through experiments.

1 Problem Description

Process optimization during the implementation of the ASHM technology encounters many challenges. The models of parts and machining tools, which are the foundation of process optimization, need to be established. In this study, the target model and machining tools need to be transformed into level set functions for process optimization. This method can effectively represent the topological change of the object through interface analysis and shape modeling. However, the complex structure of parts and the position and posture of machining tools are still challenges for implicit modeling. Meanwhile, the part orientation of WAAM is one of the critical parameters that determine the supporting structure. The supporting structure is indispensable when there is a suspended structure of the model. During the milling process, the supporting structure needs to be removed. Part orientation of the additive process needs to be optimized to minimize the support volume, reduce the manufacturing costs, and improve the surface quality. In this study, the support volume is adopted as a criterion for determining part orientation using an improved PSO algorithm. Manufacturability is another important issue; the formation quality of the target parts is sensitive to the process parameters, and the manufacturing difficulty of thin geometries and suspended structures should be fully considered. During subtractive processes, the interference between the cutting tool and the formed part should also be considered. The multiple alternations between additive and subtractive processes make the aforementioned issues more complex. The main objective of this study is to reduce the processing time and improve manufacturing efficiency while ensuring manufacturability.

2 Methodology

2.1 Implicit reconstruction

The models of the target parts and machining tools need to be built for process optimization, and the level set method is commonly applied to WAAM and has the following advantages for the research on ASHM: (1) the model of the target parts has the interface evolution and Boolean operation capabilities, which indicates that the model has strong geometric manipulability; (2) the surface area and volume of the region represented by level set functions can be calculated by the numerical integration method, which can easily determine several parameters.

The level set method uses an implicit function to describe the distribution of the target object in the 3D space and adopts the zero-equivalent contour to define the boundary of the model[16-17]. The boundary can evolve under the control of the velocity field, and the result is generally achieved by solving the Hamilton-Jacobi equation as follows:

$$\frac{\partial \Phi}{\partial T} - V^{\mathrm{n}} |\nabla \Phi| = 0 \tag{1}$$

where T is the time; V^{n} is the velocity field; Φ is the level set function of the target object after evolution. Meanwhile, the volume and surface area of the region represented by Φ can be calculated as follows:

$$V_{\Phi} = \int_{D} H(\Phi) \mathrm{d}\Omega \tag{2}$$

$$S_{\Phi} = \int_{D} \delta(\Phi) |\nabla \Phi| \mathrm{d}\Omega \tag{3}$$

where D is the design domain; Ω is the solid region of the target object; $H(\Phi)$ is the mapping process of Φ using the Heaviside function; and $\delta(\Phi)$ is the mapping process of Φ using the Dirac function. Furthermore, the volume of the intersection of any two regions Φ_{B} and Φ_{C} can be expressed as follows:

$$V_{\Phi_{\mathrm{B}} \cap \Phi_{\mathrm{C}}} = \int_{D} H(\Phi_{\mathrm{B}}) H(\Phi_{\mathrm{C}}) \mathrm{d}\Omega \tag{4}$$

The signed distance function describing the spatial distribution of the model of the target parts can be calculated, and the level set function Φ^{T} of parts can be obtained. The welding torch and cutting tools also need to be modeled by considering their structural characteristics. As shown in Fig. 1, the structures of the welding torch and cutting tool need to be simplified to measure their dimensions. Then, the level set functions of the basic graphs in the simplified diagrams can be solved. Subsequently, the Boolean operation of the level set functions is performed to obtain the level set functions Φ^{AM} and Φ^{SM} when the machining reference point is considered the origin and the tool axis coincides with the Z-axis. However, the level set functions are built under

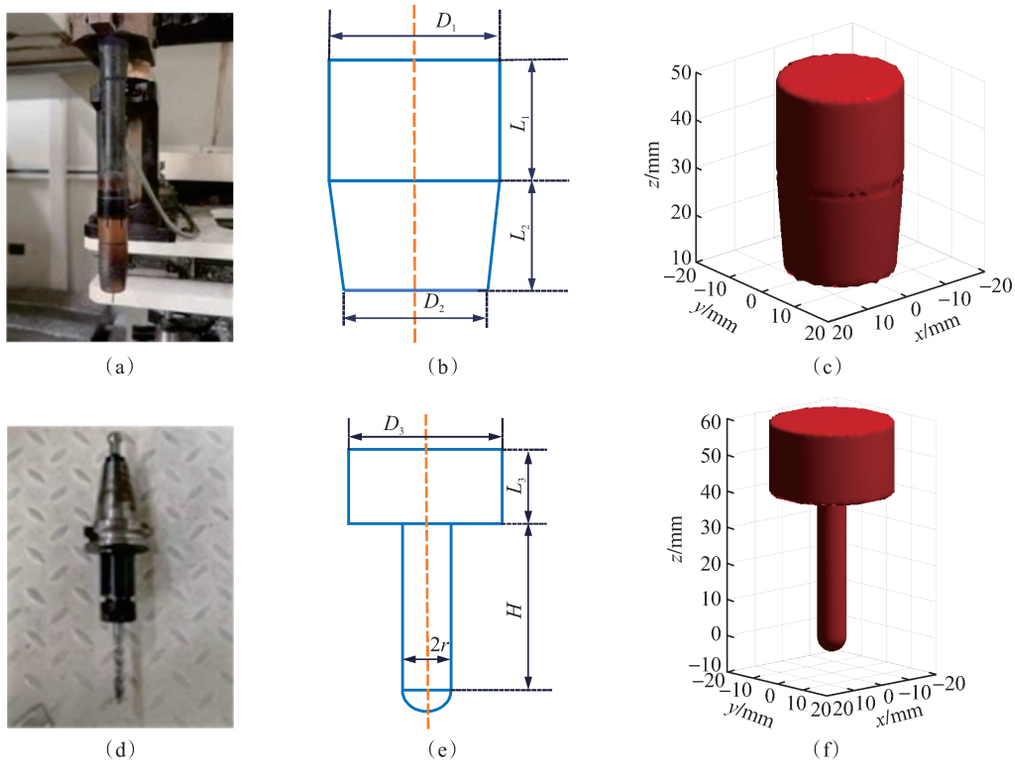

Fig. 1 Modeling process of the machining tools. (a) Actual structure of the welding torch; (b) Simplified structure of the welding torch; (c) Implicit model of the welding torch; (d) Actual structure of the cutting tool; (e) Simplified structure of the cutting tool; (f) Implicit model of the cutting tool

the local coordinate system, which should be combined with the coordinate system of the target parts in the subsequent process planning.

2.2 Part orientation optimization

The orientation needs to be determined before planning the process for the target parts to minimize the support volume and reduce manufacturing costs. In this study, the vector $\boldsymbol{d} = (x, y, z)$ is defined as a unit vector, which is equivalent to a point on the three-dimensional unit sphere s^3. Here, s is the area of the cell grid. The part orientation optimization problem for the WAAM aims to determine the direction $\boldsymbol{d}_{\mathrm{m}}$ from the unit sphere s^3 to obtain the optimal value for the objective function $f(\boldsymbol{d})$. This process can be subdivided into two key subproblems, namely, determining the specific form of the objective function $f(\boldsymbol{d})$ and solving the optimal processing direction $\boldsymbol{d}_{\mathrm{m}}$ for the WAAM.

Under the same model and process conditions and at different additive directions, the angle between each triangular facet and the horizontal plane is different; thus, the possibility of being regarded as a dangerous facet is different. The supporting area that needs to be added below the dangerous facet and the volume of the supporting structure required by the component are different. For the supporting structure that needs to be removed, when the machining parameters are fixed, the machining efficiency will only be related to the volume of the supporting structure. Therefore, the construction direction with the smallest supporting volume required is selected as the additive direction. If the angle between the triangular facet and the horizontal plane exceeds the supporting critical angle, then the triangular facet is identified as a dangerous facet, and the supporting structure needs to be added. The volume of the supporting structure can be quantitatively assessed by the volume of the space outside the model, which is located directly below the dangerous facet. As shown in Fig. 2(a), a line along the direction $\boldsymbol{d}$ is used to transpose the geometric model, and the plane passes through the nadir points of the model. Then, the obtained intersection points are sorted from bottom to top along the straight line, and the line segments between even and odd numbers (the line segments 0-1 and 2-3) are the positions where the model needs to add the supporting structure. Based on the idea of discretization, uniform meshes are generated in the plane perpendicular to the model and the construction direction, and the intersecting lines along the construction direction are arranged at the grid nodes. Then, the volume of the supporting structure can be approximately calculated by multiplying the total length of the supporting line segment by the area of the cell grid, as follows:

$$f(\boldsymbol{d}) = \sum_{i=1}^{N} \int_{0}^{l_i} s \, \mathrm{d}x \tag{5}$$

where $f(\boldsymbol{d})$ is the total volume of the supporting struc-

ture of the target model under the construction direction $\boldsymbol{d}$; l_i is the length of the i-th supporting line segment.

The improved PSO[18] is adopted to solve the optimal direction $\boldsymbol{d}_{\mathrm{m}}$. As shown in Figs. 2(b) and (c), the position of the particle is represented by the angle pair (α,β), and the increment of the angle pair $(\Delta\alpha,\Delta\beta)$ is the velocity of the particle. The rotating angles $\alpha,\beta\in[0,2\pi]$ are considered the domain of definition, and the activity range of the particle is limited to a square area with a side length 2π. If the particle is located near the boundary of the square region and the velocity vector points to the outside of the region, then the particle may cross the boundary, which leads to the divergence of the population iteration process and makes the algorithm difficult to converge. The following formula can be used to reflect the evolutionary trend of the particle when its velocity attribute is canceled:

$$P_i^{t+1}=\omega_1 P_i^t+\omega_2 P_i^{\mathrm{pb},t}+\omega_3 P^{\mathrm{gb}} \tag{6}$$

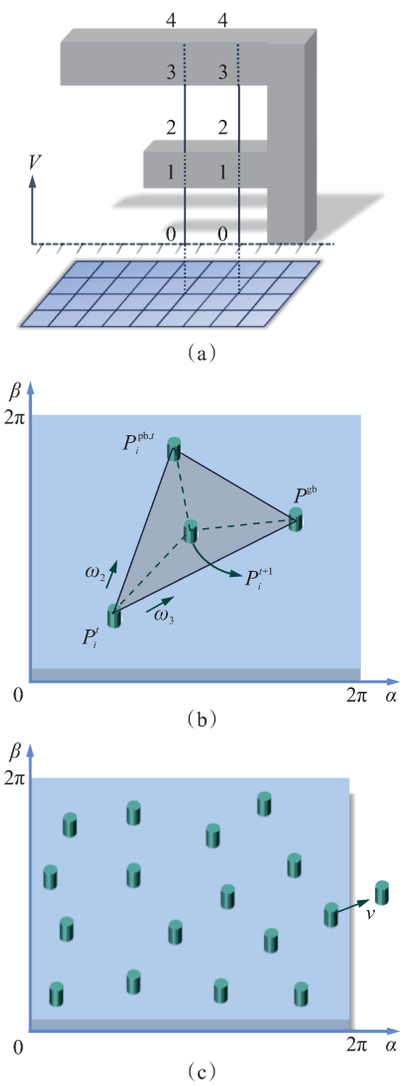

Fig. 2 Orientation optimization. (a) Determining where the support is needed; (b) Particle without the velocity property; (c) Illustration of the evolution of a particle

where P is the position of the particle, i is the sequence number of the particle, t is the number of iterations, $P_i^{\mathrm{pb},t}$ is the position of the i-th individual best particle, P^{gb} is the position of the global best particle, and ω is the weight of the particle, which is a random number in the range of $[0,1]$, and the total sum is 1. The analysis elucidates the position property and optimal behavior of the particles in the problem of the WAAM, the evolution mechanism of particles is improved, and the mutation link of the particles is added. On this basis, the optimal processing direction $\boldsymbol{d}_{\mathrm{m}}$ can be solved according to the general steps of the PSO.

2.3 Processing procedures planning

A two-step strategy is adopted to facilitate the development of the process plan. First, the model of the target parts is divided into various processing regions, and the preliminary processing sequence is formed. Then, the possible problems that may occur during the execution of the preliminary processing sequence are evaluated, and the process optimization model is established.

2.3.1 Division of the target parts

A certain number of spheres are uniformly arranged inside the target model to represent the initial subregions, and the division of the target parts is realized by the evolution of the initial subregions to fill the target parts exactly. The level set function for each initial subregion can be easily determined, and the result that the initial subregions evolve to segment the target model perfectly should meet the following conditions: (1) the union of all subregions can cover the target model completely; (2) the intersection between the union of all subregions and the nontarget region in the design domain should be empty, avoiding the extra part; and (3) any two subregions are disjointed. These requirements can be expressed as follows:

$$L_1=\int_D H(\Phi^{\mathrm{T}})\mathrm{d}\Omega-\int_D H\left(\bigcup_{i=1}^{N}\Phi_i\right)H(\Phi^{\mathrm{T}})\mathrm{d}\Omega\leqslant 0 \tag{7}$$

$$L_2=\int_D H\left(\bigcup_{i=1}^{N}\Phi_i\right)[1-H(\Phi^{\mathrm{T}})]\mathrm{d}\Omega\leqslant 0 \tag{8}$$

$$L_3=\int_D\sum_{i=1}^{N}\sum_{j=i+1}^{N}H(\Phi_i)H(\Phi_j)\mathrm{d}\Omega\leqslant 0 \tag{9}$$

where N is the number of the subregions and Φ_i is the level set function of the i-th subregion.

Then, the problem of the division of the target parts is transformed into the following model:

$$\min J=L_1+L_2+L_3 \tag{10}$$

The gradient descent method is used to solve the model. The derivative of the objective function is obtained, and according to the updated equation of the level set function, it can be known that:

$$\Phi_i'=V_i^{\mathrm{n}}|\nabla\Phi_i| \tag{11}$$

Then, the sensitivity of the objective function is obtained as follows:

$$J' = \int_D \sum_{i=1}^{N} (R_i V_i^{\mathrm{n}} |\nabla \Phi_i|) \mathrm{d}\Omega \tag{12}$$

where R_i is expanded as follows:

$$R_i = [1 - H(\Phi^{\mathrm{T}})]\delta(\tilde{\Phi}_N)\frac{\partial \tilde{\Phi}_N}{\partial \Phi_i} + \sum_{j=i+1}^{N}[H(\Phi_j)\delta(\Phi_i)] - H(\Phi^{\mathrm{T}})\delta(\tilde{\Phi}_N)\frac{\partial \tilde{\Phi}_N}{\partial \Phi_i} \tag{13}$$

Let $V_i^{\mathrm{n}} = -R_i$, and the velocity fields controlling the evolution of the initial subregions are obtained. Then, the level set functions of the subregions are updated. Finally, the subregions of the target parts are obtained.

2.3.2 Optimization of the processing procedures

The processing order of each processing region is assigned by the bottom-up logic to form the partition sequence $\{\Phi_1, \Phi_2, \cdots, \Phi_N\}$, and the processing procedure is $\{(A_1, S_1), (A_2, S_2), \ldots, (A_N, S_N)\}$, where A_i and S_i are the additive and subtractive processes in the *i*-*t*h region, respectively. For the optimization of the initial process, the manufacturability of parts during the process needs to be considered. When the additive or subtractive process is conducted for a certain region, the tool needs to smoothly process all parts of the region. The main factor affecting manufacturability is the interference between the machining tools and the area that has been formed. When the machining tools are processing a certain region, if they interfere with other parts of the model, then the processing will be hindered or even stopped. If no interference occurs, then the processing can proceed normally. Therefore, the manufacturability of the region can be evaluated by the interference between the machining tools and the formed area of the parts. Furthermore, if there is any interference, then there will be an intersection between the two. The larger the volume of the intersection is, the more difficult it is to avoid the interference. Therefore, the interference between the machining tools and the formed area of the parts can be expressed by the volume of the intersection.

When the welding torch or cutting tool processes a certain zone, its position and attitude will change with the movement of the processing point. First, the additive and subtractive processing points under the current processing region need to be determined. The welding torch and cutting tool are more likely to collide in the area that has been formed when processing the boundary of the region; thus, the surface contour of the region is discretized into points as the processing points. Then, the poses and level set functions of the machining tools at each processing point are obtained. As shown in Fig. 3 (a), the coordinate system of the initial welding torch is translated to the place where its origin coincides with the processing point of the additive process and mapping from the level set function of the welding torch to the coordinate system of the target model can be achieved. As shown in Fig. 3(b), the subtractive processing point is moved along the outside normal direction of the surface by a certain distance, which is equal to the radius of the head of the cutting tool, and the reference point of the processing point of subtractive processing can be obtained. The coordinate system of the initial cutting tool is translated to coincide with the reference point, and the axis of the cutting tool is parallel to the *Z*-axis. The coordinate system of the cutting tool is rotated around the center of the ball head to make its *Z*-axis consistent with the external normal direction of the surface. Then, the level set function model of the cutting tool under the subtractive processing point can be obtained.

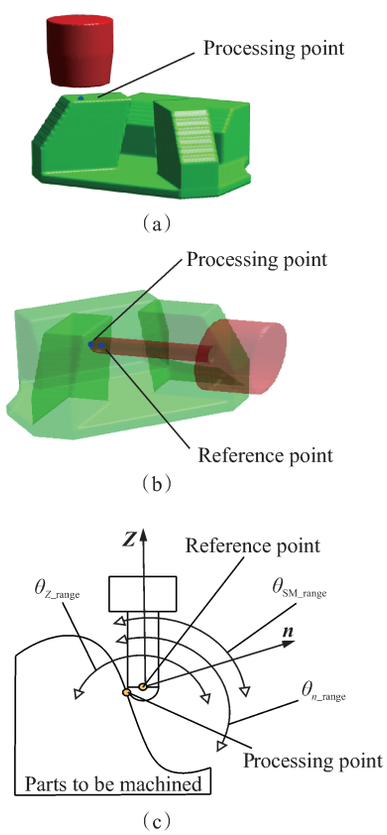

Fig. 3 Machining tools under the specified processing points. (a) Pose of the welding torch; (b) Ideal pose of the cutting tool; (c) Search for the best pose of the cutting tool

Because of the limitation of the relative motion between the machining tool and the spindle, the ideal pose of the cutting tool may not be achieved, as shown in Fig. 3(b), and adjusting the pose of the cutting tool is crucial. As shown in Fig. 3(c), the range of the angle variation of the spindle when the cutting tool is in air transport is set as θ_{Z_range}, and the normal direction outside the subtractive processing point is set as the basic direction of the axis of the cutting tool. Given that the machining effect of the subtractive processing point is poor when the angle between the actual and basic axes of the

cutting tool is large, the range of the angle variation of the actual axis relative to the basic axis of the cutting tool is set as θ_{n_range}. The range of the angle variation of the axis of the cutting tool relative to the basic axis of the cutting tool is $\theta_{SM\_range} = \theta_{Z\_range} \cap \theta_{n\_range}$. Considering the machining effect and the collision, the optimal direction of the cutting tool is selected from θ_{SM_range}, and the specific method is not introduced in detail. After determining the actual direction of the axis of the cutting tool, the rotation of the coordinate system of the cutting tool relative to the coordinate system of the model of the target parts is obtained. Based on the rotation of the coordinate system, the level set function model of the cutting tool with a reasonable pose can be obtained.

Finally, the interference volume is calculated according to Eq. (4), and the formulas for calculating the collision values of the additive and subtractive processes are respectively expressed as follows:

$$I^{AM} = \sum_{i=1}^{a} \int_D H(\Phi_i^{AM}) H(\Phi_1^*) \mathrm{d}\Omega \tag{14}$$

$$I^{SM} = \sum_{j=1}^{b} \int_D H(\Phi_j^{SM}) H(\Phi_2^*) \mathrm{d}\Omega \tag{15}$$

where a and b are the numbers of processing points of the additive and subtractive processes, respectively; Φ_i^{AM} and Φ_j^{SM} are the level set functions of the machining tools at the i-th additive processing point and the j-th subtractive processing point, respectively; Φ_1^* and Φ_2^* are the level set functions of the formed part.

Furthermore, the processing efficiency of ASHM is evaluated. The processing time is consumed by WAAM, switches of the processes, and subtractive processing. The consumed time is mainly related to the process. The time consumed by the switches of the processes is affected by the number of processes, which can be reduced by combining the processes. The time consumed by subtractive processing is influenced by the area to be processed. Under the specific division scheme of the target parts, the total milling area is roughly equal to the sum of the surface areas of each processing region. In the case of other process parameters of milling that are the same, the greater the total milling area is, the longer the subtractive processing and ASHM. Therefore, the sum of the surface contour areas of each region is used to represent the overall processing efficiency, which can be calculated as follows:

$$E = \sum_{i=1}^{N} \left[\int_D \delta(\Phi_i) |\nabla \Phi_i| \mathrm{d}\Omega \right] \tag{16}$$

The existing regions can be evolved and adjusted again to minimize the total processing area, and considering the impact of the collision, the process optimization model based on the evolution of the regions can be established as follows:

$$\min\ E = \sum_{i=1}^{N} \left[\int_D \delta(\Phi_i) |\nabla \Phi_i| \mathrm{d}\Omega \right] \tag{17}$$
$$\text{s. t.}\quad L_1 \leqslant 0, L_2 \leqslant 0, L_3 \leqslant 0, L_4 \leqslant 0, L_5 \leqslant 0$$

where L_4 is the sum of the collision values of the welding torch in all of the additive processes and L_5 is the sum of the collision values of the cutting tool in all of the subtractive processes, which can be calculated as follows:

$$L_4 = \int_D \sum_{i=2}^{N} \left\{ \left[\sum_{j=1}^{K_i} H(\Phi_j^{AM}) \right] H\left(\bigcup_{e=1}^{i-1} \Phi_e \right) \right\} \mathrm{d}\Omega \tag{18}$$

$$L_5 = \int_D \sum_{i=1}^{N} \left\{ \left[\sum_{j=1}^{Q_i} H(\Phi_j^{SM}) \right] \bigcup_{e=1}^{i} \Phi_e \right\} \mathrm{d}\Omega \tag{19}$$

where K_i and Q_i are the numbers of processing points of the i-th additive and i-th subtractive processes, respectively; $\bigcup_{e=1}^{i-1} \Phi_e$ denotes the formed part of the i-th additive process; $\bigcup_{e=1}^{i} \Phi_e$ denotes the formed part of the i-th subtractive process.

The Lagrange multiplier method is used to solve the model, and the existing partitioning scheme is optimized. However, the overswitching between additive and subtractive processes significantly affects processing efficiency, and the integration of some regions to reduce the number of processes can achieve more effective processing sequences. The method of combining regions is built based on the process combination optimization algorithm[19]:

(1) The regions in contact with the substrate are combined to form a new partition sequence, i. e., $\{\Phi_1, \Phi_2, \cdots, \Phi_{j-1}, \Phi_j, \Phi_{j+1}, \cdots, \Phi_M\}$, which is considered the sequence to be combined in subsequent rounds.

(2) Combine the adjacent regions for the sequence to be combined. For regions Φ_j and Φ_{j+1} to be combined, first, two regions are combined to form a new sequence, i. e., $\{\Phi_1, \Phi_2, \cdots, \Phi_{j-1}, \Phi_j', \Phi_{j+2}, \cdots, \Phi_M\}$; then, whether interference of the machining tools exists in the new sequence is determined. Because only region Φ_j' is affected by the combination, the method only needs to determine whether a collision of the machining tools will occur when processing the region Φ_j' according to Eqs. (16) and (17). If no collision occurs, then the combination is successful, and the new sequence is retained, j will be increased by 2, and the checked position moves back 2 bits. Otherwise, the combination is revoked, j is increased by 1, and the checked region shifts back.

(3) Determine whether j overflows; if not, execute Step 2. Otherwise, this round of the combination is ended, and a new sequence is obtained after the combination optimization. Then, Step 4 is executed.

(4) Whether the new sequence obtained is the same as the sequence to be combined at the beginning is determined. If the new sequence is the same, then there is no space for the sequence to be combined further, and the new sequence obtained is the final sequence. Otherwise,

the new sequence obtained is considered the sequence to be combined, Step 2 is executed, and the next round of combination optimization is continued.

3 Experimental Verification

The proposed method is verified by fabricating a typical model, which is a typical part with multiple branches, as shown in Fig. 4. Most of the branches of this kind of part significantly change along the extension direction in space, and the distance between the branches is small in some positions, which may lead to inaccessibility of the machining tools when the entire additive forming process is followed by subtractive processing. The inaccessibility of the machining tools is avoided by alternating the additive and subtractive processes to successfully realize the ASHM of such parts. Moreover, the extension of each branch varies considerably, and an auxiliary supporting structure may need to be added. Therefore, the orientation of the parts needs to be determined to reduce the volume of the supporting structure. As shown in Fig. 4, first, the optimal WAAM processing direction of the target object is determined. Then, as shown in Fig. 4(a), the placement posture is set as the initial state, and the volume of the required supporting structure is 238 755 mm^3. When the model is rotated 180° counterclockwise around the *Y*-axis, which is selected as the optimal placement direction, the volume of the required supporting structure is minimized to 5 328 mm^3.

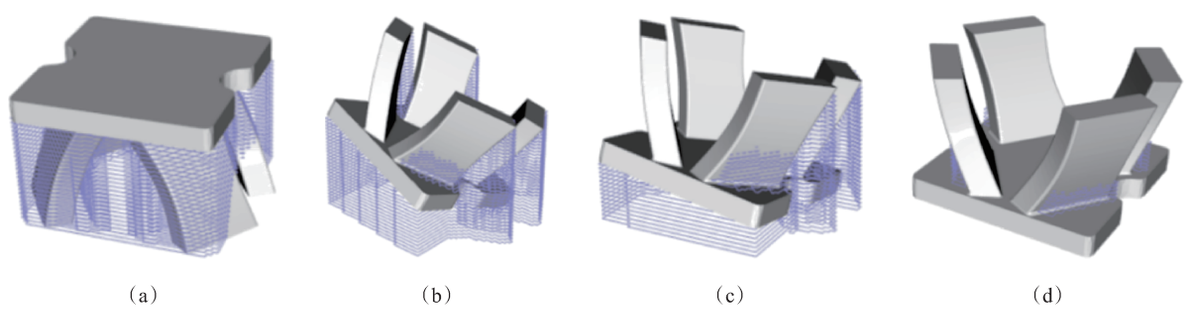

(a) (b) (c) (d)

Fig. 4 Different postures of the required supporting structure. (a) Initial state; (b) Random posture 1; (c) Random posture 2; (d) Optimal posture

As shown in Fig. 5, the example parts at the best orientation are modeled by the level set method, and a total of 16 spherical regions are arranged at the bottom of the 4 branches of the model. By solving the regional division model (Eq. (11)), the example model is divided into 16 processing regions, i.e., $\{\Phi_1, \Phi_2, \cdots, \Phi_{16}\}$, to obtain the preliminary ASHM process, i.e., $\{(A_1, S_1), (A_2, S_2), \cdots, (A_{16}, S_{16})\}$. Then, the 16 processing regions are optimized by solving the optimization model to realize the optimization of the preliminary ASHM process. Through the judgment of experience and knowledge, the preliminary process can meet the requirements of manufacturability. The preliminary processing regions are directly regarded as the optimized processing regions so that the next step of planning can be executed. Finally, the optimized processing regions are combined according to the method of process combination, and the number of the final processing regions is reduced from 16 to 4. Here, Φ_1 to Φ_8 are combined as Φ_1^*; Φ_{11} and Φ_{12} are combined as Φ_2^*; Φ_9, Φ_{10}, Φ_{13}, Φ_{14}, and Φ_{15} are combined as Φ_3^*; and Φ_{16} is left over as Φ_4^*. For the final four processing regions, interference of the machining tools will occur when further combination is performed; thus, there is no room for further combination.

The processing procedures are executed. The welding wire used for WAAM is ER5356 aluminum alloy with a diameter of 1.2 mm, and the substrate is a 6061 alumi-

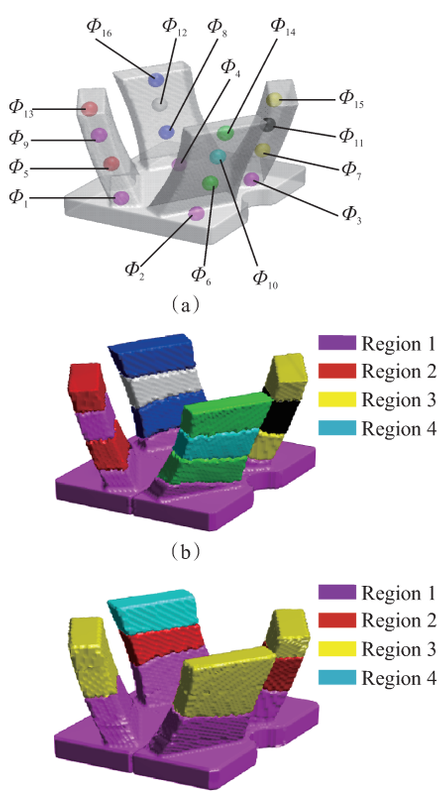

Fig. 5 Main procedures of process planning. (a) Layout of the 16 initial subregions; (b) Optimized processing regions of the target parts; (c) Final processing procedures decided by the proposed method

num plate. The wire feeding and travel speeds are 6.7 and 10 mm/s, respectively. The welding current fluctuates between 19.3 and 19.7 A. Experiments on the ASHM system are conducted, as shown in Fig. 6(a). The system is mainly composed of a cold metal transfer power source, wire feeder, driving system, headstock, tool magazine, and computerized numerical control system. The welding torch is placed in the tool magazine through a specially designed fixture. Additive and subtractive operations are alternated using different tools. The part is fixed on the rotary table, and the position and orientation are adjusted with the rotation or overturning of the rotary table. As shown in Fig. 6(b), the actual formed object is the same as the model from the perspectives of shape and size. Some defects occur at the junction of various processing regions because of the instability of WAAM, which can be eliminated by improving the processing quality. Moreover, the supporting structure used can sufficiently guarantee the normal forming of the target parts, which indicates that it is feasible to manufacture and process the target parts according to the process planning method proposed in this study.

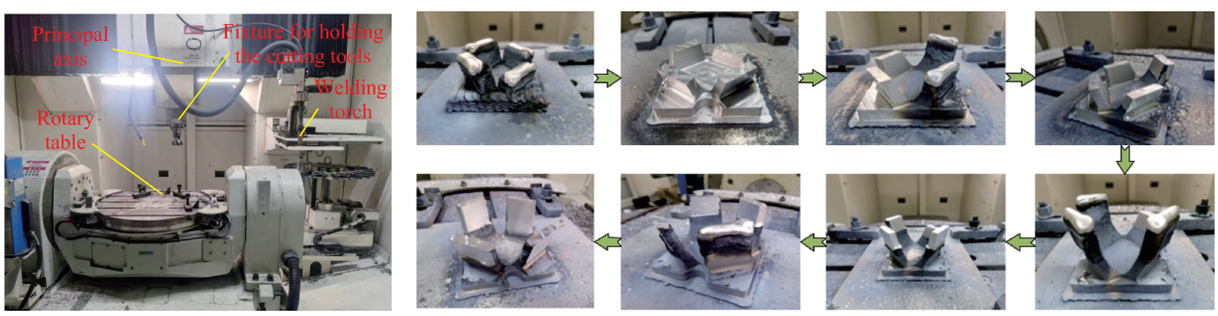

(a) (b)

Fig. 6 Verification experiment. (a) ASHM system; (b) Actual hybrid manufacturing processes

4 Conclusions

(1) The proposed methodology can effectively evaluate machining interference and manufacturing efficiency. First, the implicit models of target parts and machining tools are built by the level set method. Then, the volume of the intersection of any two regions is used as the machining interference evaluation index. Finally, the evaluation index of the manufacturing efficiency is set as the sum of the surface areas of all of the processing regions.

(2) The part orientation of the additive process is determined by the improved PSO algorithm, and the processing procedures planning method is developed based on manufacturability and manufacturing efficiency. The proposed method is verified by fabricating a typical test model. Through the analysis of the manufacturing result, the method can meet the main influencing factors in ASHM, and the application effect is passable.

(3) The proposed approach can generate alternating processing schemes for the ASHM process, which solves the problem of low efficiency and difficulty in evaluating the interference of existing methods. In the future, more characteristics (such as the thermal behavior) of WAAM will be considered in process optimization.

References

[1] SQUIRES L, ROBERTS E, BANDYOPADHYAY A. Radial bimetallic structures via wire arc directed energy deposition-based additive manufacturing [J]. Nature Communications, 2023, 14(1): 3544.

[2] CHENG J M, JIN H, ZHENG Z J, et al. Welding seam groove recognition of steel structure on construction site based on machine vision [J]. Journal of Southeast University (Natural Science Edition), 2023, 53(1): 86-93. (in Chinese)

[3] JI C, LI K, YANG T B, et al. Achieving excellent strength-ductility combination of Al-aided Mg-Gd-Al-Zr-Zn alloys fabricated by cold metal transfer-based wire-arc directed energy deposition via uniform equiaxed grains and multiple precipitates [J]. Thin-Walled Structures, 2024, 201: 111980.

[4] ZHAN J M, WU G H, TONG X, et al. Exceptional mechanical properties of wire arc additive manufactured Mg-9Gd-3Y-0.5Zr alloy induced by promoted precipitation behavior [J/OL]. Journal of Magnesium and Alloys, 2024 [2024-05-01]. https://doi.org/10.1016/j.jma.2024.01.027.

[5] ZHANG Y H, GUO Y Y, LI Z Z, et al. Effect of process parameters on microstructure and properties of arc additive manufacturing magnesium alloy [J]. Hot Working Process, 2022, 51(19): 26-29. (in Chinese)

[6] SONG G H, LEE C M, KIM D H. Investigation of path planning to reduce height errors of intersection parts in wire-arc additive manufacturing [J]. Materials, 2021, 14(21): 6477.

[7] WANG Z H, WANG J F, LIN X, et al. Effect of heat treatment on microstructure evolution and strengthening-toughening behavior of high-strength Mg-Gd-Y-Zn-Zr alloy fabricated by wire-arc additive manufacturing [J]. Journal of Materials Research and Technology, 2024, 31: 1896-1911.

[8] XIONG X C, QIN X P, JI F L, et al. Microstructure and mechanical properties of wire + arc additively manufactured mild steel by welding with trailing hammer peen-

ing[J]. Steel Research International, 2021, 92(11): 2100238.
[9] STAVROPOULOS P, BIKAS H, AVRAM O, et al. Hybrid subtractive-additive manufacturing processes for high value-added metal components[J]. The International Journal of Advanced Manufacturing Technology, 2020, 111(3): 645-655.
[10] LIU J K, HUANG J Q, ZHENG Y F, et al. Challenges in topology optimization for hybrid additive-subtractive manufacturing: A review[J]. Computer-Aided Design, 2023, 161: 103531.
[11] HARABIN G P, BEHANDISH M. Hybrid manufacturing process planning for arbitrary part and tool shapes [J]. Computer-Aided Design, 2022, 151: 103299.
[12] ZHAO Y, JIA Y Z, CHEN S J, et al. Process planning strategy for wire-arc additive manufacturing: Thermal behavior considerations [J]. Additive Manufacturing, 2020, 32: 100935.
[13] DAS A, MEDHI T, KAPIL S, et al. Different build strategies and computer-aided process planning for fabricating a functional component through hybrid-friction stir additive manufacturing[J]. International Journal of Computer Integrated Manufacturing, 2023, 37(3): 350-371.
[14] BEHANDISH M, NELATURI S, DE KLEER J. Automated process planning for hybrid manufacturing[J]. Computer-Aided Design, 2018, 102: 115-127.
[15] SOONJO K, YOSEP O. Optimal process planning for hybrid additive-subtractive manufacturing using recursive volume decomposition with decision criteria[J]. Journal of Manufacturing Systems, 2023, 71: 360-376.
[16] WEI P, LI Z Y, LI X P, et al. An 88-line Matlab code for the parameterized level set method based topology optimization using radial basis functions[J]. Structural and Multidisciplinary Optimization, 2018, 58(2): 831-849.
[17] MORI Y. Convergence proof of the velocity field for a stokes flow immersed boundary method[J]. Communications on Pure and Applied Mathematics, 2008, 61(9): 1213-1263.
[18] LI Y, ZHANG J P, HE Y Z, et al. Performance prediction of asphalt pavement based on PSO-entropy weighted unbiased grey Markov model[J]. Journal of Southeast University (Natural Science Edition), 2024, 54(2): 416-422. (in Chinese)
[19] LIU C Q, LI Y G, JIANG S, et al. A sequence planning method for five-axis hybrid manufacturing of complex structural parts[J]. Proceedings of the Institution of Mechanical Engineers, Part B: Journal of Engineering Manufacture, 2020, 234(3): 421-430.

一种新型电弧增减材混合制造工艺优化方法

郭一鸣[1], 张万元[1], 肖铭坤[1], 宋世达[2], 章晓勇[2]

(1.南京理工大学大学机械工程学院,南京 210094; 2.南京理工大学大学材料科学与工程学院,南京 210094)

摘要: 合理的工艺方案是实施电弧增减材混合制造的重要基础,提出了一种新型电弧增减材混合制造工艺优化方法。首先,利用水平集函数对目标零件和加工工具建模。其次,建立目标零件增材方向优化问题数学模型,并设计了改进粒子群优化算法以决策出最佳增材方向。然后,采用两步走策略规划目标零件的增减材混合制造交替序列,先直接将目标零件划分成各加工区域,再在考虑可制造性和制造效率的基础上优化各加工区域,并通过对加工区域的合并得到最佳混合制造交替序列。最后,采用该方法规划了所设计实例模型的工艺方案,并将其运用到模型的实际混合制造过程中。制造结果表明,该方法基本能够满足混合制造中的主要考虑点,且工艺规划过程自动化程度也较高,对人工干预的依赖较少。

关键词: 电弧增材制造;混合制造;工艺优化;可制造性

中图分类号: TH164